Long-distance entanglement of soliton spin qubits in gated nanowires

Paweł Szumniak,[1,2] Jarosław Pawłowski,[2] Stanisław Bednarek,[2] and Daniel Loss[1]
[1]*Department of Physics, University of Basel, Klingelbergstrasse 82, 4056 Basel, Switzerland*
[2]*AGH University of Science and Technology, Faculty of Physics and Applied Computer Science, al. Mickiewicza 30, 30-059 Kraków, Poland*
(Received 15 January 2015; revised manuscript received 4 June 2015; published 2 July 2015)

We investigate numerically the charge, spin, and entanglement dynamics of two electrons confined in a gated semiconductor nanowire. The electrostatic coupling between electrons in the nanowire and the induced charge on the metal electrodes leads to a self-trapping of the electrons, which results in solitonlike properties. We show that the interplay of an all-electrically controlled coherent transport of the electron solitons and of the exchange interaction can be used to realize ultrafast SWAP and entangling $\sqrt{\text{SWAP}}$ gates for distant spin qubits. We demonstrate that the latter gate can be used to generate a maximally entangled spin state of spatially separated electrons. The results are obtained by quantum-mechanical time-dependent calculations with exact inclusion of electron-electron correlations.

DOI: 10.1103/PhysRevB.92.035403 PACS number(s): 73.21.La, 03.67.Lx, 73.63.Nm

I. INTRODUCTION

One of the most striking manifestations of the quantum laws of physics is entanglement [1,2]. The ability to entangle qubits is also an essential ingredient for quantum computation [3]. The spins of electrons confined in an array of electrostatically defined quantum dots (QD) emerged as a promising candidate for encoding quantum bits of information [4,5]. Spin qubits weakly interacting with their environment can be electrically controlled and show potential in scalability [6]. Recent experiments have demonstrated fast and precise manipulation, initialization, and measurement of spin qubits confined in lateral QDs [7–15] and nanowire QDs [16]. Furthermore, long spin decoherence times have been reported, reaching $\sim$ 200 ns [16] for InAs QDs and $\sim$270 μs [17] for GaAs QDs, and the charge noise has been measured to be very weak $\sim$1 μV [18].

However, the ability to couple and entangle solid state spin qubits over long distances, which is essential for realizations of scalable quantum computer architectures and for applications of fault-tolerant quantum error correction (QEC) schemes, still seems to be one of the key challenges to overcome. The first encouraging steps toward coupling remote spin qubits via microwave cavities [19–21] have been recently reported [21–23]. Coherent long-range spin qubit coupling based on cotunneling phenomena [24] has been demonstrated for an array consisting of three quantum dots [25,26]. There are also several interesting proposals for coupling spatially separated QD spin qubits, e.g., using ferromagnets [27], floating gates [28], Majorana edge modes [29–31], or superconductors [32]. Cooper-pair splitters may be another promising source for nonlocal spin-entangled electrons [33–36]. Another interesting platform useful for coupling spin qubits are mobile electrons shuttled by surface acoustic waves [37–39] or flying qubits [40], however, spin entanglement of such moving electrons has not been reported so far.

In this paper, we propose an all-electrically controlled and ultrafast method for realization of the SWAP and $\sqrt{\text{SWAP}}$ gates and for generating maximally entangled spin states of spatially separated electrons. Our scheme does not require coupling with an additional external system—"quantum bus"—which may simplify its implementation. The proposed scheme is based on the interplay between the exchange interaction and theoretically proposed on-demand coherent transport [41] of self-trapped electron solitons [42,43] confined in gated semiconductor nanostructures. Exchange interaction, which has a short-range character, limits the ability to couple spatially separated spin qubits confined in stationary QDs. However, for mobile electron solitons, this is not the case. Self-trapping allows for transporting spatially separated initially not entangled electrons to the region where they can entangle their spins due to the exchange interaction and finally be separated and transported back to distant regions as an entangled entity. To be specific, we present the results for structurally defined InAs nanowires. However, one can expect qualitatively similar results for electrostatically defined quantum wires in 2DEG/2DHG systems as proposed, e.g., in Refs. [41], and for different materials. The main difference will be in the timing but qualitatively the results will be the same. One can integrate the proposed SWAP and $\sqrt{\text{SWAP}}$ gates with all-electrically controlled single ultrafast quantum logic gates [44], which can be arranged in a 2D scalable register (Ref. [45]) and be selectively manipulated. Such an architecture may be particularly suitable for implementation of powerful QEC surface codes [46].

II. MODEL

We consider two electrons confined in an InAs semiconductor nanowire covered by seven electrodes e_L, e_R, e_J, and e_{1-4}, to which the voltages $V_{L,R,J,1-4}$ are applied [47], respectively. The radius of the nanowire is $l = 5$ nm. The nanowire is separated from the metal by a dielectric material (InAlAs) [48], and the distance from the center of the nanowire to the metal is $d = 15$ nm. The presented system can be described by the quasi-1D Hamiltonian

$$H = \sum_{j=1,2}\left[\frac{p_j^2}{2m} + V_{\text{conf}}(x_j,\rho(x,t))\right] + V_C^{1D}(x_1,x_2) + H_{\text{BR}}, \tag{1}$$

where $p_j = -i\hbar\partial/\partial x_j$ is the x component of the momentum operator for the jth electron, $j = 1,2$, $m = 0.023m_0$ is the effective mass of the electrons confined in the InAs nanowire,

and m_0 is the free electron mass. The two-electron wave function is represented as

$$\Psi(x_1,x_2,t) = \begin{pmatrix} \psi_{\uparrow\uparrow}(x_1,x_2,t) \\ \psi_{\uparrow\downarrow}(x_1,x_2,t) \\ \psi_{\downarrow\uparrow}(x_1,x_2,t) \\ \psi_{\downarrow\downarrow}(x_1,x_2,t) \end{pmatrix}. \quad (2)$$

It has to be antisymmetric with respect to simultaneous exchange of the space and spin coordinates: $\psi_{ij}(x_1,x_2,t) = -\psi_{ji}(x_2,x_1,t)$, where $i,j = \uparrow, \downarrow$ indicate the spin projections of the first and the second electron on the z axis.

The electrons in the nanowire induce a positive charge on the surface of the metal electrodes, which in turn leads to the self-confinement of the electron wave function along the wire. This wave function has solitonlike properties [42,43]: it can be transported in the form of a stable wave packet that maintains its shape while traveling. Moreover, it can reflect or pass through obstacles (potential barriers or wells) with 100% probability while preserving its shape. This effect can be exploited to realize on-demand transport of self-confined electrons, whose motions can be fully controlled by geometry and voltages applied to the electrodes [41]. The binding energy of such solitons depends on m, ε-dielectric constant, and on d (electron-metal distance) [43]. Most favorable conditions for the soliton observation are expected for semiconductors with large m, small ε, and short distance d ($\leqslant$20 nm). For InAs with $d = 15$ nm, the binding energy is ~ 1 meV. Thus we expect that at sub-Kelvin temperatures thermal excitations will not destroy the soliton effects. We note that similar self-trapping effects have been reported for vacuum/metal or dielectric/metal interfaces [49–51].

In the general case (e.g., arbitrary geometry of the electrodes), the induced self-confining potential is determined using the Poisson-Schrödinger self-consistent scheme, which was described in detail in Refs. [41]. However, since in the considered structure the electrodes form almost uniform wide plates (the interelectrode distance is about 10 nm), in order to determine the induced potential, we can use instead the image charge technique [43,52–54],

$$V_{\text{ind}}(x,t) = \frac{e}{4\pi\varepsilon\varepsilon_0}\int dx' \frac{\rho(x',t)}{\sqrt{(x-x')^2+4d^2}}. \quad (3)$$

This greatly simplifies and speeds up the numerical calculations. Quantum calculations within linear response theory [43,55] indicate that it is a good approximation for the actual response potential of the electron gas. Here, $\varepsilon = 14.3\varepsilon_0$ for InAs nanowires [56]. In stark contrast to the commonly used pointlike approximations of the image charge, we take here into account the spatial distribution of the image charge in a direction parallel to the metal plate. The two-electron charge density is defined as

$$\rho(x,t) = e\int dx'(|\Psi(x,x',t)|^2 + |\Psi(x',x,t)|^2), \quad (4)$$

where $|\Psi(x_1,x_2,t)|^2 = \sum_{i,j=\uparrow,\downarrow}|\psi_{ij}(x_1,x_2,t)|^2$. The voltages applied to the electrodes generate an additional electrostatic potential in the nanowire region, $\phi_0(x,y_0,z_0)$, which we determine by solving the Laplace equation, $\nabla^2\phi_0(x,y,z) = 0$, under the conditions $\phi_0(x,y_{\text{gates}},z) = V_i$, where V_i is the voltage applied to the ith electrode. Thus, according to the superposition principle, the total confinement potential for the electrons in the nanowire can be expressed as

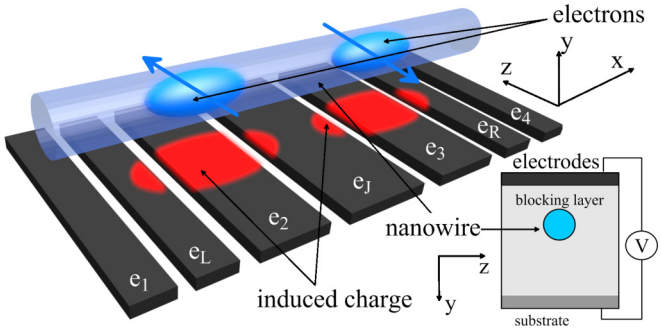

FIG. 1. (Color online) Schematic view of the nanostructure and its cross-section. The nanowire is covered by seven electrodes which are labeled by e_{1-4} and $e_{L,R,J}$. Two electrons with opposite spins (blue arrows) are confined in the nanowire. The positive charge induced on the gate surface is marked by red areas.

$$V_{\text{conf}}(x,\rho(x,t)) = -|e|V_{\text{ind}}(x,t) - |e|\phi_0(x,y_0,z_0). \quad (5)$$

The electric field E_y, generated by the electrodes, and the induced charges is also the source of the Bychkov-Rashba spin-orbit interaction (SOI) in the nanowire, $H^j_{\text{BR}} = \alpha E_y k_{x_j}\sigma_z$ [57]. The corresponding BRSO Hamiltonian for the two electrons in the quasi-1D nanowire takes the form $H_{\text{BR}} = H^1_{\text{BR}}\otimes I + I\otimes H^2_{\text{BR}}$. However, for a chosen orientation of the electrodes, wire, and initial electron spin (either up or down along the z direction) the motion of the electrons along the wire does not induce spin rotations, but slightly increases spin swap times. Furthermore, we assume that the nanowire is grown along the [111] crystallographic direction, which allows us to neglect the Dresselhaus SOI [56], which can affect weakly the gate fidelity [58].

The effective 1D Coulomb interaction between electrons in a nanowire with strong parabolic confinement in the y and z directions has the form [59]

$$V_C^{1D}(x_1,x_2) = \frac{1}{\sqrt{2\pi}4\varepsilon_0\varepsilon l}\text{erfcx}\left(\frac{|x_1-x_2|}{\sqrt{2}l}\right). \quad (6)$$

The time evolution of the system is described by the nonlinear time-dependent Schrödinger equation $i\hbar\frac{\partial}{\partial t}\Psi(x_1,x_2,t) = H\Psi(x_1,x_2,t)$, which we solve numerically using an explicit Askar-Cakmak scheme [60]. As initial condition we take the ground state $\Psi(x_1,x_2,t_0) = \Psi_0(x_1,x_2)$ for the two self-confined electrons under the metal electrodes, which we obtain by solving the eigenvalue equation $H\Psi_0(x_1,x_2) = E\Psi_0(x_1,x_2)$ with the imaginary time propagation method [61]. In this approach, electron-electron correlations are taken into account exactly.

To characterize the properties of the system, we evaluate the spin density (ith component) of the two-electron system,

$$\rho_{S_i}(x,t) = \frac{\hbar}{2}\int_{x_L}^{x_R} dx'(\Psi^\dagger(x,x',t)\sigma_i\otimes I\Psi(x,x',t) + \Psi^\dagger(x',x,t)I\otimes\sigma_i\Psi(x',x,t)), \quad (7)$$

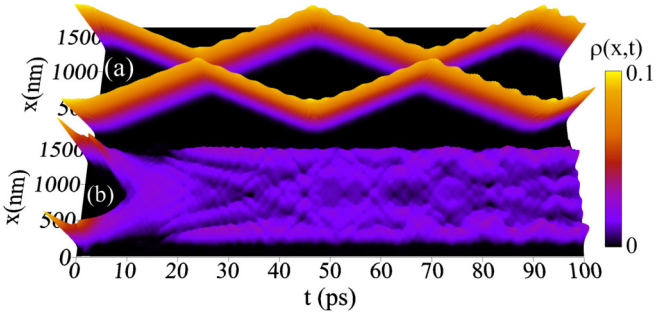

FIG. 2. (Color online) Time evolution of the charge density $\rho(x,t)$ illustrating the difference in propagation and collision of two incident electrons between the case with (a) and without (b) image charge potential. Note the self-trapping and the solitonlike behavior in case (a).

where σ_i is ith Pauli matrix, $i = x,y,z$. Consequently, with this formula, the expectation value of the electron spin in the left (s_z^L) or right (s_z^R) part of the nanostructure takes the form

$$s_z^{L(R)}(t) = \int_{x_L(x_0)}^{x_0(x_R)} dx \rho_{S_z}(x,t), \tag{8}$$

where x_0 is the midpoint of the nanowire and x_L (x_R) denotes the left (right) end of the nanowire. The amount of entanglement between the spin in the left and the right parts of the nanowire can be quantified by calculating the concurrence [62], which is defined as $C(\rho^{S_{LR}}) = \max\{0, \sqrt{\lambda_1} - \sqrt{\lambda_2} - \sqrt{\lambda_3} - \sqrt{\lambda_4}\}$. It varies from zero for completely separable (nonentangled) states to unity for maximally entangled states. Here, λ_i are eigenvalues (in decreasing order) of $\tilde{\rho} = \rho^{S_{LR}}(\sigma_y \otimes \sigma_y)\rho^{S_{LR}*}(\sigma_y \otimes \sigma_y)$. The $\rho^{S_{LR}}$ is the reduced density matrix for two-electron spin states in the left and right parts of the nanowire:

$$\rho^{S_{LR}} = 2\int_{x_L}^{x_0} dx_1 \int_{x_L}^{x_R} dx_2\, \rho(x_1,x_2,x_1,x_2), \tag{9}$$

where $\rho(x_1,x_2,x_1,x_2) = |\Psi(x_1,x_2)\rangle\langle\Psi(x_1,x_2)|$ is the full two-electron density matrix. In the above definition of reduced density matrix $\rho^{s_{LR}}$, we take into account the double occupancy of electron states in the right and left part of the nanowire.

III. RESULTS

First, we investigate the charge dynamics and illustrate differences in propagation between self-trapped solitonlike electrons and "freely" propagating electrons not interacting with the metal. Initially, electrons are confined in the nanowire under the electrodes e_L and e_R (see Fig. 1), which is achieved by applying $V_{1,2,3,4} = -1$ meV and zero voltage to the other gates $V_{L,R,J} = 0$. The electrons are forced to move against each other by changing the voltage on electrodes $e_{2,3}$ to $V_{2,3} = 0$ and by lowering the voltage on electrodes $e_{1,4}$ to $V_{1,4} = -1.5$ mV [63]. The time evolution of the two-electron charge density $\rho(x,t)$ along the wire is depicted in Fig. 2. It can be seen that the electrons being self-trapped under the metal maintain their charge density shape while moving, which is a characteristic feature of soliton waves. Furthermore, the shape is not affected by the collision with other electrons [Fig. 2(a)].

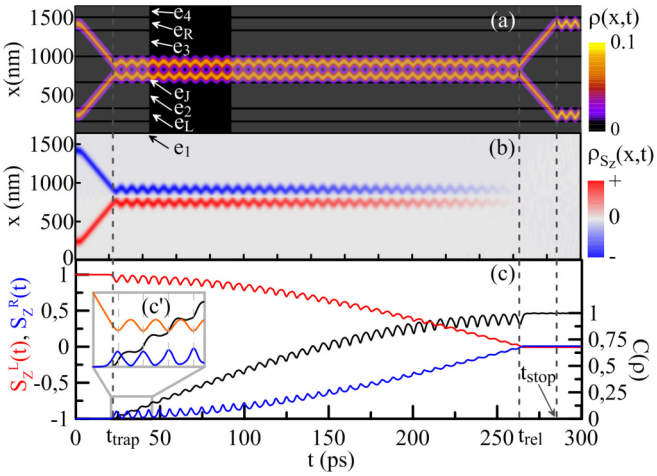

FIG. 3. (Color online) (a) Time evolution of the charge density $\rho(x,t)$ and scheme of the electrodes covering the nanodevice (grey). Time evolution of (b) the z component of spin density ρ_{S_z} and (c) the z component of the expectation value of the electron spin in the left $s_L(t)$ (red) and the right $s_R(t)$ (blue) part of the nanowire (referred to the left axis). The concurrence C (black) of the two-electron spin state is shown with respect to the right axis in (c). In the inset (c′) of Fig. 3(c), we plot the average distance $|x_1 - x_2|$ (orange) between electrons for the first few collisions.

However, this is not the case for "free" electrons that are not interacting with the metal [Fig. 2(b)] [64].

In order to realize a quantum $\sqrt{\text{SWAP}}$ gate using the nanodevice from Fig. 1, we propose the following scheme. Initially (for t_0), each of the electrons is localized under spatially separated (by about 1.2 μm) electrodes e_L and e_R, in a spin-up $s_z^L(t_0) = \hbar/2$ and a spin-down $s_z^R(t_0) = -\hbar/2$ state, respectively. Thus the initial state has the following form [65]: $\Psi_0(x,y) = (0, \varphi_L(x_1)\varphi_R(x_2), -\varphi_R(x_1)\varphi_L(x_2), 0)^T$, where $\varphi_R(x_i)$ and $\varphi_L(x_i)$ are the single electron ground-state orbitals localized in the right (R) and in the left (L) dot. In this situation, there is no entanglement, i.e., $C(\rho(t_0)) = 0$.

Then, by changing the voltage on the electrodes (in the same manner as in the previous example), the electrons start to move. When the electrons reach the region under the electrode e_J (for $t = t_{\text{trap}} \approx 20$ ns), the voltage on the neighboring electrodes $e_{2,3}$ is set to $V_{2,3} = -1$ mV, which traps the electrons under e_J. Then the electrons collide periodically under this electrode. The time evolution of the charge (zth component of spin) density for the two electrons $\rho(x,t)$ [$\rho_{S_z}(x,t)$] is plotted in Fig. 3(a) [Fig. 3(b)]. The time evolution of the expectation value of the spin in the left and right part of the nanodevice and the concurrence C is depicted in Fig. 3(c). During each collision (due to exchange interaction which is intrinsically present in our model), electrons exchange a fraction of the spin and consequently entanglement builds up between electron spins in the left and right part of the nanodevice. This is illustrated in Fig. 3(c′) where we also plot the average distance between electrons (orange line). Dips in the average value of the spin or concurrence are due to a local and temporary increase of double occupation probability [66] during the soliton collision.

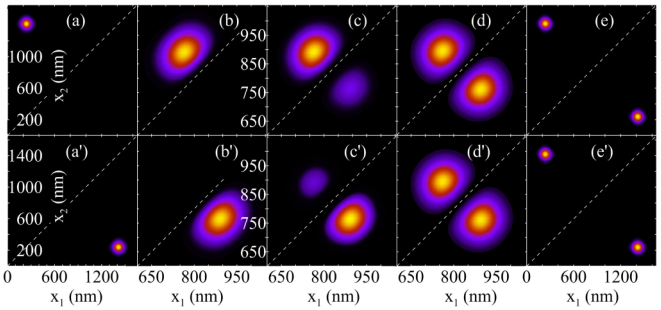

FIG. 4. (Color online) Probability densities of the two-electron wave functions $|\psi_{\uparrow\downarrow}(x_1,x_2,t)|^2$ (upper panel) and $|\psi_{\downarrow\uparrow}(x_1,x_2,t)|^2$ (lower panel with primes) for the instants (a) t_0, (b) $t_{\rm trap}$, (c) $t_{1/2}$ $[C(\rho(t_{1/2}))=0.5]$, (d) $t_{\rm rel}$, and (e) $t_{\rm stop}$ during the realization of the $\sqrt{\rm SWAP}$ gate.

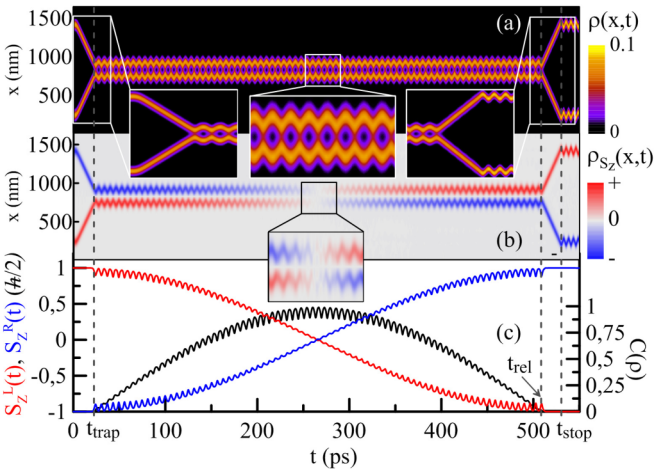

FIG. 5. (Color online) Same as Fig. 3 but for the SWAP gate.

After many collisions, for $t \approx 260$ ps, we have a situation where the spin density vanishes and the spin in the left and the right dot is equal to zero, $s_z^L(t) \approx s_z^R(t) \approx 0$. Furthermore, the concurrence reaches $C(\rho(t)) \approx 1$, which indicates that the spins are maximally entangled. However, the system is not yet in the spatially separated entangled state. In order to separate electrons from the area under the electrode e_J, the voltage on the electrodes $e_{2,3}$ is switched (for $t_{\rm rel} \approx 260$ ps) to $V_{2,3}=0$, and after the last collision, the electrons start to move into opposite directions. When they reach the region under the electrodes $e_{L,R}$ (initial position) for $t_{\rm stop} \approx 280$ ps, respectively, they are trapped again by changing the voltage on electrodes $e_{1,2,3,4}$ to $V_{1,2,3,4}=-2$ mV. Finally, the maximally spin-entangled state is obtained for spatially separated electrons characterized by the concurrence reaching $C(\rho) > 0.999$.

It is also instructive to analyze the probability densities of the components of the total two-electron wave functions during the entanglement generation process. For the chosen initial state with opposite spins, during the whole evolution, components with parallel spins are zero $\psi_{\uparrow\uparrow}=\psi_{\downarrow\downarrow}=0$, while the other two are nonzero. The corresponding values $|\psi_{\uparrow\downarrow}(x_1,x_2,t)|^2$ and $|\psi_{\downarrow\uparrow}(x_1,x_2,t)|^2$ are depicted in Fig. 4 for the initial moment t_0—nonentangled spatially separated electrons, $t_{\rm trap}$—first collision, $t_{1/2}$ when the concurrence becomes $C(\rho(t_{1/2}))=0.5$, $t_{\rm rel}$ last collision when the electron spins are maximally entangled, and finally for the maximally entangled and separated electron spins under electrodes $e_{L,R}$.

A similar procedure can be used to realize the two-qubit SWAP gate, which fully exchanges the spin of the two electrons. In this case, electrons have to be released from under the electrode e_J for $t_{\rm rel} \approx 510$ ps and trapped again under $e_{L,R}$ for $t_{\rm stop} \approx 530$ ps. The results are shown in Fig. 5. It is clearly seen how electrons exchange their spins during soliton collisions under electrode e_J. It is quite remarkable that despite many collisions the shape of the electron wave function (charge density) is still preserved and well localized.

The difference between voltages on gate e_L, e_R, and neighboring gates determines the initial electron momentum and thus $t_{\rm trap}$. The larger the voltage difference the higher the momentum and the shorter $t_{\rm trap}$ become. The switching times $t_{\rm trap}$ and $t_{\rm stop}$ have to be tuned with about ± 4 ps precision in order to properly trap electrons. Such precise tuning, however, can be avoided altogether by allowing the soliton to dissipate energy. The kinetic energy of the electron (initially transferred to it) can be absorbed, e.g., by interaction with an electron gas from a nearby quantum well via retardation effects [55]. Only $t_{\rm rel}$ needs to be tuned in this case, where even a 30% deviation from $t_{\rm rel}$ is allowed and the concurrence reaches still more than 90%.

The operation times τ_{op} of the proposed gates are on the order of hundreds of picoseconds, which is three orders of magnitude shorter than the reported spin decoherence time in InAs QDs [16]. However, one can further tune (decrease) the gate operation time by increasing the voltage applied to the gates $e_{3,4}$.

IV. CONCLUSION

We have shown that the interplay of solitonlike properties of mobile self-trapped electrons in gated semiconductor nanowires and the exchange interaction can be exploited to realize ultrafast (subnanoseconds) SWAP and $\sqrt{\rm SWAP}$ gates for remote spin qubits. The latter gate can be used to realize maximally entangled spin states of spatially separated electrons. The proposed gates are all electrically controlled which makes our proposal particularly suitable for scalability purposes. Furthermore, the mobile character of entangled electron spins can be useful for the realization of quantum teleportation in solid state nanostructures.

ACKNOWLEDGMENTS

We acknowledge support from the Swiss SNF, NCCR QSIT, SCIEX (P.S.), and IARPA. S.B. has been supported by National Science Centre, Poland, under Grant No. UMO-2014/13/B/ST3/04526.

[1] A. Einstein, B. Podolsky, and N. Rosen, Phys. Rev. **47**, 777 (1935).

[2] R. Horodecki, P. Horodecki, M. Horodecki, and K. Horodecki, Rev. Mod. Phys. **81**, 865 (2009).

[3] M. Nielsen and I. Chuang, *Quantum Computation and Quantum Information*, Cambridge Series on Information and the Natural Sciences (Cambridge University Press, Cambridge, 2000).

[4] D. Loss and D. P. DiVincenzo, Phys. Rev. A **57**, 120 (1998).

[5] D. D. Awschalom, L. C. Bassett, A. S. Dzurak, E. L. Hu, and J. R. Petta, Science **339**, 1174 (2013).

[6] C. Kloeffel and D. Loss, Ann. Rev. Condensed Matter Phys. **4**, 51 (2013).

[7] J. Petta, A. Johnson, J. Taylor, E. Laird, A. Yacoby, M. Lukin, C. Marcus, M. Hanson, and A. Gossard, Science **309**, 2180 (2005).

[8] F. Koppens, C. Buizert, K.-J. Tielrooij, I. Vink, K. Nowack, T. Meunier, L. Kouwenhoven, and L. Vandersypen, Nature (London) **442**, 766 (2006).

[9] E. A. Laird, C. Barthel, E. I. Rashba, C. M. Marcus, M. P. Hanson, and A. C. Gossard, Phys. Rev. Lett. **99**, 246601 (2007).

[10] R. Brunner, Y.-S. Shin, T. Obata, M. Pioro-Ladrière, T. Kubo, K. Yoshida, T. Taniyama, Y. Tokura, and S. Tarucha, Phys. Rev. Lett. **107**, 146801 (2011).

[11] M. D. Shulman, O. E. Dial, S. P. Harvey, H. Bluhm, V. Umansky, and A. Yacoby, Science **336**, 202 (2012).

[12] A. P. Higginbotham, F. Kuemmeth, M. P. Hanson, A. C. Gossard, and C. M. Marcus, Phys. Rev. Lett. **112**, 026801 (2014).

[13] Z. Shi, C. B. Simmons, D. R. Ward, J. R. Prance, X. Wu, T. S. Koh, J. K. Gamble, D. E. Savage, M. G. Lagally, M. Friesen, S. N. Coppersmith, and M. A. Eriksson, Nat. Commun. **5**, 3020 (2014).

[14] M. Veldhorst, J. Hwang, C. Yang, A. Leenstra, B. de Ronde, J. Dehollain, J. Muhonen, F. Hudson, K. Itoh, A. Morello, and S. Dzurak, Nat. Nanotechnol. **9**, 981 (2014).

[15] J. Yoneda, T. Otsuka, T. Nakajima, T. Takakura, T. Obata, M. Pioro-Ladrière, H. Lu, J. Palmstrøm, A. C. Gossard, and S. Tarucha, Phys. Rev. Lett. **113**, 267601 (2014).

[16] S. Nadj-Perge, S. Frolov, E. Bakkers, and L. P. Kouwenhoven, Nature (London) **468**, 1084 (2010); S. Nadj-Perge, V. S. Pribiag, J. W. G. van den Berg, K. Zuo, S. R. Plissard, E. P. A. M. Bakkers, S. M. Frolov, and L. P. Kouwenhoven, Phys. Rev. Lett. **108**, 166801 (2012); J. W. G. van den Berg, S. Nadj-Perge, V. S. Pribiag, S. R. Plissard, E. P. A. M. Bakkers, S. M. Frolov, and L. P. Kouwenhoven, *ibid.* **110**, 066806 (2013).

[17] H. Bluhm, S. Foletti, I. Neder, M. Rudner, D. Mahalu, V. Umansky, and A. Yacoby, Nat. Phys. **7**, 109 (2011).

[18] A. V. Kuhlmann, J. Houel, A. Ludwig, L. Greuter, D. Reuter, A. D. Wieck, M. Poggio, and R. J. Warburton, Nat. Phys. **9**, 570 (2013).

[19] G. Burkard and A. Imamoglu, Phys. Rev. B **74**, 041307 (2006).

[20] M. Trif, V. N. Golovach, and D. Loss, Phys. Rev. B **77**, 045434 (2008).

[21] P.-Q. Jin, M. Marthaler, A. Shnirman, and G. Schön, Phys. Rev. Lett. **108**, 190506 (2012).

[22] T. Frey, P. J. Leek, M. Beck, A. Blais, T. Ihn, K. Ensslin, and A. Wallraff, Phys. Rev. Lett. **108**, 046807 (2012).

[23] K. Petersson, L. McFaul, M. Schroer, M. Jung, J. Taylor, A. Houck, and J. Petta, Nature (London) **490**, 380 (2012).

[24] P. Stano, J. Klinovaja, F. R. Braakman, L. M. K. Vandersypen, and D. Loss, arXiv:1409.4852.

[25] F. Braakman, P. Barthelemy, C. Reichl, W. Wegscheider, and L. Vandersypen, Nat. Nanotechnol. **8**, 432 (2013).

[26] M. Busl, G. Granger, L. Gaudreau, R. Sánchez, A. Kam, M. Pioro-Ladrière, S. Studenikin, P. Zawadzki, Z. Wasilewski, A. Sachrajda, and P. G., Nat. Nanotechnol. **8**, 261 (2013); R. Sánchez, G. Granger, L. Gaudreau, A. Kam, M. Pioro-Ladrière, S. A. Studenikin, P. Zawadzki, A. S. Sachrajda, and G. Platero, Phys. Rev. Lett. **112**, 176803 (2014).

[27] L. Trifunovic, F. L. Pedrocchi, and D. Loss, Phys. Rev. X **3**, 041023 (2013).

[28] L. Trifunovic, O. Dial, M. Trif, J. R. Wootton, R. Abebe, A. Yacoby, and D. Loss, Phys. Rev. X **2**, 011006 (2012).

[29] P. Bonderson and R. M. Lutchyn, Phys. Rev. Lett. **106**, 130505 (2011).

[30] M. Leijnse and K. Flensberg, Phys. Rev. Lett. **107**, 210502 (2011); Phys. Rev. B **86**, 104511 (2012).

[31] S. Plugge, A. Zazunov, P. Sodano, and R. Egger, Phys. Rev. B **91**, 214507 (2015).

[32] M.-S. Choi, C. Bruder, and D. Loss, Phys. Rev. B **62**, 13569 (2000); M. Leijnse and K. Flensberg, Phys. Rev. Lett. **111**, 060501 (2013).

[33] P. Recher, E. V. Sukhorukov, and D. Loss, Phys. Rev. B **63**, 165314 (2001).

[34] L. Hofstetter, S. Csonka, J. Nygård, and C. Schönenberger, Nature (London) **461**, 960 (2009).

[35] J. Schindele, A. Baumgartner, and C. Schönenberger, Phys. Rev. Lett. **109**, 157002 (2012).

[36] A. Schroer, B. Braunecker, A. Levy Yeyati, and P. Recher, Phys. Rev. Lett. **113**, 266401 (2014).

[37] V. I. Talyanskii, J. M. Shilton, M. Pepper, C. G. Smith, C. J. B. Ford, E. H. Linfield, D. A. Ritchie, and G. A. C. Jones, Phys. Rev. B **56**, 15180 (1997).

[38] S. Hermelin, S. Takada, M. Yamamoto, S. Tarucha, A. Wieck, L. Saminadayar, C. Bauerle, and T. Meunier, Nature (London) **477**, 435 (2011); R. McNeil, C. Kataoka, M Ford, C. Barnes, D. Anderson, G. Jones, I. Farrer, and D. Ritchie, *ibid.* **477**, 439 (2011).

[39] H. Sanada, Y. Kunihashi, H. Gotoh, K. Onomitsu, M. Kohda, J. Nitta, P. Santos, and T. Sogawa, Nat. Phys. **9**, 280 (2013).

[40] M. Yamamoto, S. Takada, C. Bäuerle, K. Watanabe, A. D. Wieck, and S. Tarucha, Nat. Nanotechnol. **7**, 247 (2012).

[41] S. Bednarek, B. Szafran, R. J. Dudek, and K. Lis, Phys. Rev. Lett. **100**, 126805 (2008).

[42] K. Yano and D. K. Ferry, Superlattices Microstruct. **11**, 61 (1992).

[43] S. Bednarek, B. Szafran, and K. Lis, Phys. Rev. B **72**, 075319 (2005).

[44] S. Bednarek and B. Szafran, Phys. Rev. Lett. **101**, 216805 (2008).

[45] P. Szumniak, S. Bednarek, J. Pawłowski, and B. Partoens, Phys. Rev. B **87**, 195307 (2013).

[46] R. Raussendorf and J. Harrington, Phys. Rev. Lett. **98**, 190504 (2007); D. S. Wang, A. G. Fowler, and L. C. L. Hollenberg, Phys. Rev. A **83**, 020302 (2011).

[47] Since the metal gate is in contact with an undoped semiconductor, the Schottky barrier V_B should be taken into account with sub mV accuracy. Therefore the potential applied to the gates is equal to $V_i \rightarrow V_i + V_B$. V_B should be determined experimentally for a certain structure.

[48] We assume that the value of the dielectric constant of the material surrounding the nanowire is equal or close to that of the nanowire.
[49] D. F. Padowitz, W. R. Merry, R. E. Jordan, and C. B. Harris, Phys. Rev. Lett. **69**, 3583 (1992).
[50] N.-H. Ge, C. Wong, R. Lingle, J. McNeill, K. Gaffney, and C. Harris, Science **279**, 202 (1998).
[51] A. D. Miller, I. Bezel, K. J. Gaffney, S. Garrett-Roe, S. Liu, P. Szymanski, and C. Harris, Science **297**, 1163 (2002).
[52] A. Hartstein and Z. Weinberg, J. Phys. C **11**, L469 (1978).
[53] A. Hartstein, Z. A. Weinberg, and D. J. DiMaria, Phys. Rev. B **25**, 7174 (1982).
[54] M. I. Chibisov and A. V. Roitman, J. Exp. Theor. Phys. **89**, 129 (1999).
[55] S. Bednarek and B. Szafran, Phys. Rev. B **73**, 155318 (2006).
[56] R. Winkler, *Spin-Orbit Coupling Effects in Two-Dimensional Electron and Hole Systems*, 191 (Springer, Berlin, 2003).
[57] E. I. Rashba, Sov. Phys. Solid State **2**, 1109 (1960); Y. A. Bychkov and E. I. Rashba, J. Phys. C **17**, 6039 (1984).
[58] M. P. Nowak and B. Szafran, Phys. Rev. B **82**, 165316 (2010).
[59] S. Bednarek, B. Szafran, T. Chwiej, and J. Adamowski, Phys. Rev. B **68**, 045328 (2003).
[60] A. Askar and A. S. Cakmak, J. Chem. Phys. **68**, 2794 (1978).
[61] K. Davies, S. Flocard, H. Krieger, and M. S. Weiss, Nucl. Phys. A **342**, 111 (1980).
[62] S. Hill and W. K. Wootters, Phys. Rev. Lett. **78**, 5022 (1997); W. K. Wootters, *ibid.* **80**, 2245 (1998).
[63] Voltage fluctuations on the electrodes should be at least one order of magnitude smaller than the voltage difference between the gates in order not to affect electron soliton motion and formation.
[64] The freely propagating wave packet with initial Gaussian form: $\psi(x,t=0)=(\sqrt{2\pi}\sigma_0)^{-0.5}\exp[-x^2/4\sigma_0^2+ip_0x]$ evolve in time as $\psi(x,t)=(\sqrt{2\pi}\sigma(t))^{-1}\exp[-(x-\hbar p_0 t/m)^2/2\sigma^2(t)]$. Its "width" $\sigma(t)$ grows linearly in time as $\hbar t/2m\sigma_0^2$ according to $\sigma(t)=\sigma_0\sqrt{1+\hbar^2t^2/4m^2\sigma_0^4}$, which indicates rapid spreading of the wave packet.
[65] J. Pawłowski, P. Szumniak, A. Skubis, and S. Bednarek, J. Phys. Condens. Matter **26**, 345302 (2014).
[66] J. Schliemann, D. Loss, and A. H. MacDonald, Phys. Rev. B **63**, 085311 (2001).